Inhibition of the Mammalian Target of Rapamycin Pathway Stimulates Osteoblast Proliferation and Differentiation Through Autophagy in MC3T3-E1 Cells

Xining Li
Huzhou University https://orcid.org/0000-0002-6544-5057
Xi-Ning Li
Huzhou University
Yu Zhao
Huzhou University
Zhi-Gang Zhou
The first affiliated hospital of Huzhou University
Hong-Chang Zhou
Huzhou University
Ji-Kang Min (2504074093@qq.com)
Huzhou University https://orcid.org/0000-0003-2612-9833

Research

Keywords: Osteoporosis, Autophagy, Mammalian target of rapamycin (mTOR), Proliferation, Differentiation

Posted Date: June 29th, 2020

DOI: https://doi.org/10.21203/rs.3.rs-36977/v1

Abstract

Background: OP(Osteoporosis) is a common bone metabolic disorder in the elderly characterized by loss of bone mass and a tendency to fracture. The mammalian target of rapamycin (mTOR) pathway in autophagy plays an indispensable role in maintaining the stability of the intracellular environment and ensuring the normal physiological functions of cells.

Methods: In this study, different concentrations(20, 40, 60, 80, 100, 120, 140, 160, 180 and 200nM) of rapamycin were used to act on MC3T3-E1 osteoblasts for different time lengths(6, 12, 24, 36 and 48 hours). CCK8 was used to detect the proliferative activity of cells and screen suitable rapamycin concentration for subsequent experiments. Western blot and real-time quantitative PCR were used to detect the expression changes of phosphorylated mTOR, upstream and downstream mTOR pathway, autophagy and osteogenic differentiation markers. The expression of LC3 was observed by immunofluorescence. The differentiation ability of osteoblasts was observed by alizarin red and alkaline phosphatase staining.

Results: The results showed that the induction of proliferation activity of osteoblasts from 20 nM to 200 nM presented a parabolic feature. After the action time of 50 μM rapamycin exceeded 12 hours, the proportion of S stage cells was significantly increased. The results of gene and protein analysis showed that rapamycin significantly inhibited the phosphorylation of mTOR, and the phosphorylation of the downstream factors of mTOR, 4E-BP1(eIF4E-binding protein 1) and S6K1(p70 ribosomal S6 kinase 1) also decreased. Rapamycin significantly increased the expression of LC3 II (microtubule associated protein 1 light chain 3-α), significantly increased the ratio of LC3II/LC3I, and significantly decreased the expression of p62(sequestosome-1). Rapamycin significantly induced the expression of ALP(Alkaline phosphatase), Runx2(Runt-related transcription factor 2) and osterix.

Conclusions: This study confirmed that rapamycin stimulates the autophagy of osteoblasts by inhibiting mTOR and promotes their proliferation and differentiation, suggesting that mTOR may be a potential therapeutic target for osteoporosis.

Background

Osteoporosis (OP) is a progressive and systemic bone metabolic disease, which is featured by bone mass loss, bone fragility and propensity to fracture (1). The incidence of OP has been increasing yearly due to population aging (2,3). Absent early symptoms and signs are one major feature of OP in clinical practice (4). For this reason, people affected by OP are very likely to suffer osteoporotic fracture, restricted mobility after fracture and other complications. Basic research has shown that the bone marrow mesenchymal stem cells, osteoblasts and osteoclasts are jointly involved in the pathogenesis of OP. The bone is in a dynamic balance of bone formation and absorption. A close coordination between the osteoblasts, osteoclasts, hormones and other factors is required for maintaining bone homeostasis (5). It

has been shown that osteoblast apoptosis is enhanced by aging, and reduced bone matrix synthesis resulting from lower osteoblast differentiation is the main mechanism of OP (6).

Autophagy is a highly conservative behavior in eukaryotic cells, which is closely related to cellular homeostasis and stress, damage repair, proliferation and differentiation (7). Autophagy plays an important role in maintaining intracellular homeostasis and normal physiological functions of cells (8). Among the molecular studies of cellular autophagy, the mammalian target of rapamycin (mTOR) signaling pathway is most intensively discussed. mTOR participates in a variety of biological processes, including cell development, ribosome formation and metabolic regulation (9). mTORC1 induces the phosphorylation of ULK1-ATG13-ATG101-FIP200 complex, leading to its inactivation (10). repamycin activates ULK1 by inhibiting mTORC1, thereby enhancing the activity of the Beclin1-VPS34-ATG14L-p150 complex and triggering autophagy (11). It has been found that the mTORCl activity in osteoclast precursor cells promotes proliferation of osteoblasts, but inhibits their differentiation (12). Other reports have indicated that raptor knockout in osteoblast precursor cells leads to suppressed mTORC1 activity, along with reduced trabecular bones and thinned cortical bones (13).

A growing body of evidence seems to show that autophagy is involved in the regulation of bone metabolism, proliferation, differentiation, metabolism and physiological functions of bone marrow mesenchymal stem cells and osteoblasts (14). ATG7 and the wingless/int1 (Wnt) signaling pathway are involved in the BMP-2-induced early formation of osteoblasts. BMP-2 promotes the expression of ATG7, but LC3, Beclin1 and ATG5 are not affected. After ATG7 and Wnt16 are silenced by small interfering RNA, the BMP-2-mediated differentiation of human skeletal muscle stem cells into osteoblasts is significantly inhibited In contrast, the autophagy agonist repamycin dramatically enhances the osteogenic differentiation of hSMSCs, indicating that autophagy promotes early differentiation of osteoblasts (15). Although autophagy has been proven to regulate osteoblast differentiation, the specific mechanism remains unclear. The purpose of the present study was to verify whether the mTOR signaling pathway promoted osteoblast differentiation by inducing autophagy.

Materials And Methods

Cell culture

MC3T3-E1 cells (Cell bank of the Chinese Academy of Sciences, Shanghai, China) were grown in Dulbecco's modified Eagle's medium (high glucose; Gibco; Thermo Fisher Scientific, Inc., Waltham, MA, USA) supplemented with 10% fetal bovine serum (Gibco; Thermo Fisher Scientific) and penicillin-streptomycin solution (100 U/mL penicillin; 100 µg/mL streptomycin; Gibco; Thermo Fisher Scientific), in a humidified atmosphere with 5% CO^2 at 37°C.

Cell viability assay

Cell viability assessment was performed using a Cell Counting Kit-8 (CCK-8, Signalway Antibody, MD, USA). MC3T3-E1 cells (1×10^4/well) were seeded in 96-well plates, incubated overnight and then treated with rapamycin at various concentrations 20, 40, 60, 80, 100, 120, 140, 160, 180 and 200 nM for 6, 12, 24, 36 and 48 hours. Cell viability was determined by CCK-8. Ten microliters of CCK-8 reagent were added to each well and incubated at 37°C for 3 h, until the media turned yellow. Absorbance was measured at 450 nm in a spectrophotometer.

Analysis of the cell cycle

A Cell Cycle Detection kit (KeyGen Biotech Co. Ltd, Nanjing, China) was used to assess the cell cycle. Following treatment with 50 nM rapamycin for 48 hours, the MC3T3-E1 cells were trypsinized, collected and washed with PBS. Subsequently, 70% cold ethanol was added to fix the cells for 2 h at room temperature or overnight at 4°C, and PBS was used to wash away the fixing solution. Cells were incubated with 0.4 mL PI containing 0.1 mL RNase A at 37°C for 30 min. Finally, cell cycle distribution was analyzed by measuring the DNA content using a flow cytometer.

Western blot analysis

The protein level were determined by Western blotting. MC3T3-E1 osteoblasts were seeded into 100 mm dishes and cultured in complete α-MEM to 70% confluency, following which the cells were treated with 50 nM rapamycin for 6, 12, 24, 36 and 48 hours. Total proteins were extracted following lysis of the cells in RIPA buffer at 4°C for 1 h. The lysates were centrifuged at 20000 rpm for 30 min, and the protein concentration was determined using a BCA protein quantification kit. Equal amounts of protein (30 μg) were loaded into each well of a 7.5–15% SDS-PAGE gel and transferred to PVDF membranes (Millipore Corp., Bedford, MA, USA). Membranes were incubated overnight at 4°C with the primary antibodies p62 (1:1000), LC3-II (1:1000), mTOR (1:1000), p-mTOR (1:1000), 4E-BP1 (1:1000), p-4E-BP1 (1:1000), S6K1 (1:1000), p-S6K1 (1:1000), Akt (1:1000), p-Akt (1:2000), phosphatidylinositol 3-kinase (PI3K) (1:1000), runt-related transcription factor 2 (Runx2) (1:1000), GAPDH (1:3000) (Cell Signaling Tehnology, Beverly, MA, USA), osterix (1:1000), and alkaline phosphatase (ALP) (1:1000) (Santa Cruz Biotechnology, Santa Cruz, CA, USA). Adding secondary antibody (goat anti-rabbit IgG-HRP, 1:5000, Santa Cruz) incubated for 2 h. The specific bands were visualized using an enhanced chemiluminescence detection system (Thermo Fisher Scientific) and imaged with an Alpha Imager HP (ProteinSimple, San Jose, CA, USA). The band density was quantified using the ImageJ image processing program (National Institutes of Health, Bethesda, MD, USA. software version 1.5b).

Immunofluorescence staining

MC3T3-E1 osteoblasts were seeded in 24-well plates with culture slides (Beyotime Institute of Biotechnology, Shanghai, China) and upon reaching 50% confluency, were treated with 50 nM rapamycin

for 12, 24, 36 and 48 hours. The cells were washed twice with PBS, fixed with 4% paraformaldehyde at room temperature for 15 min, and permeabilized with 0.5% Triton X-100 for 2 min at room temperature. After blocking for 2 h with 5% bovine serum albumin (Beyotime Institute of Biotechnology) at room temperature, the cells were incubated overnight with anti-LC3-II antibody (1:200) at 4°C. After 1 h incubation with Fluorescein (FITC)-conjugated secondary antibody (1:5000) (Santa Cruz), the cells were counterstained with DAPI for 10 min at room temperature. The stained cells were imaged using confocal fluorescence microscopy (magnification, ×200, DS-U3 Nikon Eclipse CI; Nikon Corporation, Tokyo, Japan).

Reverse transcription and real-time PCR

MC3T3-E1 osteoblasts were seeded at a density of 5×10^4 cells/well in 100 mm dishes for 3 days until the cells reached 70% confluence. The cells were treated with 50 nM rapamycin for 6, 12, 24, 36 and 48 hours as described, and total RNA was extracted using TRIzol® reagent (Invitrogen; Thermo Fisher Scientific), according to the manufacturer's protocol. Total RNA was extracted and quantified by scanning spectrophotomer. A total of 1 μg of RNA was used in the reverse transcription reaction using RevertAid First Strand cDNA Synthesis Kit (Thermo Fisher Scientific) according to the manufacturer's protocols. For gene-specific primed cDNA synthesis, the reaction was conducted for 60 min at 42°C. Then, for random hexamer primed synthesis, incubate for 5 min at 25°C. RT was terminated by heating at 70°C for 5 min. Real-time PCR was performed using the SYBR Green PCR Master Mix (Applied Biosystems; Thermo Fisher Scientific) on the ABI 7500 Fast Real-Time PCR System (Applied Biosystems 7500 System Sequence Detection System, software version 2.6.2; Thermo Fisher Scientific, Inc.). The PCR conditions were as follows: 95°C preheating for 1 min, followed by 40 cycles of 95°C for 15 s (denaturation), 60°C for 20 s (annealing), and 72°C for 32 s (elongation). Glyceraldehyde-3-phosphate dehydrogenase (GAPDH) was used as the inner reference. The threshold cycle (Ct) values were calculated using the StepOnePlus system software (Applied Biosystems). The relative expression of each mRNA was calculated by the $2^{-(\Delta Ct)}$ method. The primer sequences were as follows: LC3-II forward 5'-CCGACCGCTGTAAGGAGG-3'; LC3-II reverse 5'-AAGCCGAAGGTTTCTTGGGA-3'; p62 forward 5'-GTGTGCCCAGACTACGACCT-3'; p62 reverse 5'-GACTCAGCTGTAGGGCAAGG-3; mTOR forward 5'-CGCTACTGTGTCTTGGCATC-3'; mTOR reverse 5'-GGTTCATGCTGCTTAGTCGG-3'; ALP forward 5'-TGCCCTGAAACTCCAAAAGC-3'; ALP reverse 5'-CTTCACGCCACACAAGTAGG-3; Runx2 forward 5'-CCCAGCCACCTTTACCTACA-3'; Runx2 reverse 5'-TATGGAGTGCTGCTGGTCTG-3; osterix forward 5'-CATCCCTATGGCTCGTGGTA-3'; osterix reverse 5'-TGGGTTAAGGGGAGCAAAGT-3'; GAPDH forward 5'-ATGGGTGTGAACCACGAGA-3'; GAPDH reverse 5'-CAGGGATGATGTTCTGGGCA-3'.

Statistical analysis

All statistical tests were performed by SPSS20.0 statistics software (SPSS, Chicago, USA). All experiments were performed three times. Values are expressed as the mean ± standard deviation (SD). Differences between two groups were analyzed by the LSD and Duncan's test. Independent samples t test

or one-way analysis of variance was used in comparison between groups. All statistical analysis was performed using SPSS for Windows ver. 19.0 (IBM Corp., Armonk, NY, USA). $p<0.05$ was considered to indicate a statistically significant difference.

Results

Rapamycin stimulates the proliferation activity of MC3T3-E1 osteoblasts

The effect of rapamycin (20, 40, 60, 80, 100, 120, 140, 160, 180 and 200 nM) on MC3T3-E1 cell viability was viewed in Figure 1. The results showed that there was no significant change in cell proliferation activity when rapamycin was used for 6 h. From the beginning of 12 h, rapamycin above 20 nm significantly promoted the proliferation of osteoblasts ($p<0.05$, $p<0.01$, respectively). With the increase of rapamycin concentration, the proliferation promoting effect of rapamycin on osteoblasts gradually decreased. The results showed that rapamycin had two-way effect on osteoblasts, which was promoted by low to medium concentration and inhibited by high concentration. According to the above experimental results, 50 nM rapamycin was selected as the subsequent induction condition.

Rapamycin increases the ratio of S-phase in MC3T3-E1 osteoblasts

The cell cycle of each group was determined by flow cytometry. When 50 nM rapamycin was added, compared with the ratio of MC3T3-E1 cell in the control group (75.5% in G1 phase and 7.9% in S-phase), the cell ratio in G1 phase in the rapamycin group was reduced significantly (67.3% at 12 h, 63.8% at 36 h and 67.3% at 48 h) ($p<0.05$), and that in S-phase was increased (20.0% at 12 h, 18.4% at 24 h, 27.4% at 36 h and 28.8% at 48 h) ($p<0.05$, $p<0.01$, respectively), suggesting that rapamycin can promote MC3T3-E1 cells from G1 phase to S phase and promote cell division and proliferation (Figure 2A and 2B).

Rapamycin inhibits the mTOR signaling pathway in MC3T3-E1 osteoblasts

PI3K-Akt-mTOR is a classical autophagy signaling pathway, and rapamycin is an inhibitor of mTOR. After the action of 50 nM rapamycin in MC3T3-E1 cells, the expression of mTOR in cells was significantly reduced ($p<0.01$), and the longer the interaction time, the lower the phosphorylation level of mTOR. At the same time, rapamycin also resisted the upstream pathway of mTOR, which showed that the expression of PI3K was significantly decreased in the induction groups ($p<0.01$), and the phosphorylation of Akt was inhibited, and the expression of p-Akt was significantly decreased ($p<0.05$, $p<0.01$, respectively). These results indicated that rapamycin negatively regulate the phosphorylation of PI3K/Akt/mTOR in MC3T3-E1 cells (Figure 3A and 3B). After mTOR activation, it mainly regulates the downstream factors of 4EBP1

and S6K1. After 50 nM rapamycin was applied to MC3T3-E1 cells, the phosphorylation level of mTOR in the cells gradually decreased with the extension of the action time, while the phosphorylation levels of its downstream 4EBP1 and S6K1 were significantly reduced (Figure 4A and 4B).

Rapamycin stimulates autophagy in MC3T3-E1 osteoblasts

To analyze the effects of rapamycin on autophagy in MC3T3-E1 osteoblasts, the cells were treated with 50 nM rapamycin, and various autophagy markers LC3-II and p62 were detected. The ratio of LC3-II/LC3-I is frequently analyzed to determine the extent of autophagy. After 6 hours of 50 nM rapamycin treatment, the LC3-II conversion rate of osteoblasts increased steadily, and the expression of LC3-II was significantly enhanced. The LC3-II/LC3-I ratio increased significantly with the extension of rapamycin treatment time, and p62 showed a significant decreasing trend ($p<0.05$, $p<0.01$, respectively). In the action time node of rapamycin, only 12 h showed special performance, and rapamycin significantly inhibited the formation of LC3-II ($p<0.05$) (Figure 5A and 5B). Furthermore, immunofluorescence staining of cells treated with rapamycin was carried out to detect the colocalization of LC3-II, and the results showed that in addition to the decrease in the fluorescence intensity of LC3-II at 12 h, the fluorescence intensity of LC3-II was significantly increased at 24 h after rapamycin treatment, and the number of apoptotic bodies in circular green fluorescence was significantly increased (Figure 6A–6E). To further clarify the effects of rapamycin on autophagy, changes in the gene expressions of LC3-II, p62 and mTOR were detected by qRT-PCR. The results showed that the gene expressions of mTOR and p62 were obviously inhibited by rapamycin compared with control ($p<0.05$, $p<0.01$, respectively). LC3-II was significantly increased except 48 h group ($p<0.05$, $p<0.01$, respectively) (Figure 7). These results demonstrated that rapamycin stimulated autophagy in MC3T3-E1 osteoblasts.

Rapamycin promotes MC3T3-E1 osteoblast differentiation

To detect the function of rapamycin in osteoblast differentiation, western blot assay and real-time quantitative PCR were used to detect the expression of transcription factors related to osteoblast differentiation including ALP, Runx2 and osterix. Treatment with 50 nM rapamycin significantly increased ALP activity ($p<0.01$), except 12 h group. The enhancement of ALP activity was concentration dependent on rapamycin. In addition to 12 h group, rapamycin also promoted the expression of Runx2 and osterix ($p<0.05$, $p<0.01$, respectively) (Figure 8A and 8B). The specific performance of rapamycin in 12 h was consistent with its effect on the autophagy marker LC3-II. By further gene expression detection, ALP, Runx2 and osterix were expressed in the same direction as protein level, and rapamycin significantly induced ALP, Runx2 and osterix expression at the gene level ($p<0.05$, $p<0.01$, respectively) (Figure 9). ALP can be stained with calcium and cobalt to form black deposits in the cells, which can be used to observe the activity of alkaline phosphatase in osteoblasts. The results showed that with the extension of rapamycin treatment time from 6 h to 48 h, the black precipitation of osteoblasts increased and the alkaline phosphatase staining gradually deepened (Figure 10). Further, alizarin red S staining was used to

observe the formation of mineralized nodules in osteoblasts induced by rapamycin. The results showed that after 12 d of rapamycin action, significant mineralized nodules could be observed in the cells, and a few calcium salt crystals could be observed at 2 d and 6 d (Figure 11). These results indicated that rapamycin enhanced osteoblast differentiation.

Discussion

External stimuli (e.g., ischemia, hypoxia, brain damage and convulsion) may induce autophagy, whereby the cells clear way the intracellular damaged organelles and other waste components (16). Autophagic regulation implicates several complex processes, where mTOR, Beclin1, Ca^{2+} and PI3K signaling pathways are involved (17). mTORCl activity plays an important role in autophagosome formation and maturation, while repamycin blocks the mTORCl-mediated autophagy (18). After the mTORC1 activity is strengthened, S6K1 is phosphorylated and activated, which further induces the phosphorylation of P70S6 and promotes mRNA translation (19). Meanwhile, migration of ribosomes to the endoplasmic reticulum is accelerated, thereby promoting the adhesion of ribosomes to the endoplasmic reticulum. This further prevents ribosome falling off the endoplasmic reticulum, thereby promoting the maturation of the autophagic membrane (19,20). Given the facts above, autophagy is regulated by the mTORCl signaling pathway. Autophagy is involved in several pathological and physiological processes of human organs (21,22). However, the roles played by autophagy in bone homeostasis and metabolism remain to be further investigated. MC3T3-E1 osteoblasts are usually used to investigate the osteogenic features of bone differentiation and mineralization, which are appropriate for research about the molecular mechanism of osteoblast maturation and extracellular matrix formation (23). In the present study, MC3T3-E1 cells were used to observe the osteogenic features and the induction of autophagy by repamycin in osteoblasts.

Osteoblasts were treated with different concentrations of rapamycin and proliferation of osteoblasts was detected with the cck-8 kit. Cell cycle changes were measured using a cell cycle assay kit. The results showed that with the increase of rapamycin concentration, the proliferation of osteoblasts increased significantly, and the reverse inhibition was observed after a certain concentration was exceeded. Changes in cell cycle are related to concentration. The higher the concentration of rapamycin was, the higher the proportion of cells entering S phase from G1 phase, indicating that rapamycin promoted the proliferation of osteoblasts.

The PI3K/Akt/mTOR pathway is an important intracellular signaling pathway regulating autophagy and cell cycle, and it is directly related to cell dormancy, proliferation, carcinogenesis and lifespan (24,25). PI3K activation induces the phosphorylation and activation of Akt, which is localized at the cytoplasm (26). The signal is transmitted to the downstream via Akt, activating mTOR (27,28). The results showed that repamycin, as an mTOR inhibitor, significantly inhibited the phosphorylation of mTOR. Meanwhile, the phosphorylation of the Akt signaling pathway upstream of mTOR was inhibited evidently, while the expression level of Akt itself remained unchanged. The PI3K expression was also downregulated to a

great extent. The experiment showed that repamycin not only inhibited the mTOR activity, but also suppressed the activity of Akt.

During the process of autophagic formation, the cytoplasmic material enveloped by the double-sided membrane is called autophagosome (29,30). Autophagosomes bind to lysosomes to degrade the relevant cytoplasmic structures (31). The primary autophagy proteins involved in autophagosome formation are ATG5, beclin-1 and LC3, the early changes of which may influence the subsequent bone development process (32,33). In recent years, more experiments seem to demonstrate that the osteoblast differentiation is accompanied by upregulated LC3II and SQSTM1/p62, although the interaction between the two is less known (34). The LC3II/LC3I ratio can be used to detect the generation of autophagic flux. After lipidization, LC3 undergoes a transformation from LC3I to LC3II, and the lipidated LC3 is considered as a marker for autophagosome formation (35). The present study proved the repamycin -mediated transformation from LC3I to LC3II at the genetic and protein levels, with a significant increase in the LC3II/LC3I ratio. Moreover, the degradation of p62 was increased, indicating that repamycin significantly induced the autophagy of osteoblasts. The expression levels of osteogenic markers ALP, Runx2 and osterix were detected to determine osteoblast differentiation (36). Results showed that with the addition of repamycin into the osteoblasts, the expressions of ALP, Runx2 and osterix were increased significantly at the genetic and protein levels. Under the action of rapamycin ALP staining obviously deepened, the formation of mineralized nodules, late show that rapamycin targeted by inhibiting mTOR phosphorylation, also inhibit the upstream pathways Akt phosphorylation at the same time, to enhance the osteoblast autophagy level, role in early and late all can promote the osteoblast differentiation, prompting mature osteoblast, strengthen the osteogenetic activity.

Conclusion

Our study demonstrated that rapamycin significantly inhibited the phosphorylation of mTOR and Akt, thereby blocking the activation of mTOR downstream pathway 4EBP1 and S6K1, while enhancing the level of autophagy in osteoblasts. The proliferation and differentiation of osteoblasts were also improved. However, the key downstream molecules related to autophagy are not yet identified, and other pathways may be involved. Moreover, animal experiments may be required to clarify this issue. Our experiment only demonstrates that autophagy may be correlated with bone metabolic diseases, such as OP. Taken together, it was found that repamycin promoted osteoblast differentiation while inducing osteoblast autophagy, indicating that autophagy may be a potential target for the treatment of OP.

Declarations

Acknowledgements

Not applicable.

Competing interests

The authors declare that they have no conflict of interest.

Authors' contributions

XNL and JKM were involved in developing the concept and design of the study, and are guarantors of the integrity of the study. XNL and HCZ performed the experiments, prepared and revised the manuscript. YZ and ZGZ were responsible for the literature review and assisted with data analysis. All authors have read and approved the final version of the manuscript submitted for publication.

Funding

This work was supported by grant from Youth Program of National Natural Science Foundation of China (81602805), Key Laboratory of Vector Biology and Pathogen Control of Zhejiang Province, Huzhou University (Grant No. HUZUL201910) and the Natural Science Foundation of Zhejiang Province, China (Grant No. GF19H060008).

Availability of data and materials

The datasets generated and analyzed during the present study are available from the corresponding author on reasonable request.

Ethics approval and consent to participate

Not applicable.

Patient consent for publication

Not applicable.

References

1. Bisson EJ, et al. Multiple sclerosis is associated with low bone mineral density and osteoporosis. Neurol Clin Pract. 2019;9(5):391-9.
2. Kessler K, et al. Meal timing, aging, and metabolic health. Int J Mol Sci. 2019;20(8):1911.
3. Kristof Major, et al. Unknown osteoporosis in older patients admitted to post-acute rehabilitation. Aging Clin Exp Res. 2020;32(6):1145-52.
4. Aspray TJ, et al. Osteoporosis and the ageing skeleton. Subcell Biochem. 2019;91:453-76.
5. Shen G, et al. Autophagy as a target for glucocorticoid-induced osteoporosis therapy. Cell Mol Life Sci 2018; 75(15):2683-93.
6. Singh L, et al. Good, bad, or ugly: the biological roles of bone marrow fat. Curr Osteoporos Rep. 2018; 16(2):130-37.

7. Buszczak M, et al. Autophagy keeps the balance in tissue homeostasis. Dev Cell. 2019;49(4):499-500.
8. Nakashima A, et al. Role of autophagy in oocytogenesis, embryogenesis, implantation, and pathophysiology of pre-eclampsia. J Obstet Gynaecol Res. 2017;43(4):633-43.
9. Choi J, Jo M, Lee E, Choi D. AKT is involved in granulosa cell autophagy regulation via mTOR signaling during rat follicular development and atresia. Reproduction. 2013;147(1):73-80.
10. Switon K, et al. Molecular neurobiology of mTOR. Neuroscience. 2017;341:112-53.
11. Noda T. Regulation of autophagy through TORC1 and mTORC1. Biomolecules. 2017;7(3):52.
12. Chen J , et al. mTORC1 signaling promotes osteoblast differentiation from preosteoblasts. PLoS One. 2015;10(6):e0130627.
13. Xie F, et al. Conditional knockout of raptor/mTORC1 results in dentin malformation. Front Physiol. 2019;10:250.
14. Grosso R, et al. Autophagy: a necessary event during erythropoiesis. Blood Rev. 2017;31(5):300-5.
15. Ozeki N, et al. Bone morphogenetic protein-induced cell differentiation involves Atg7 and Wnt16 sequentially in human stem cell-derived osteoblastic cells. Exp Cell Res. 2017;347(1):24-41.
16. Smith CM, et al. Autophagy in acute brain injury: feast, famine, or folly? Neurobiol Dis. 2011;43(1):52-9.
17. Nikoletopoulou V, et al. Crosstalk between apoptosis, necrosis and autophagy. Biochim Biophys Acta. 2013;1833(12):3448-59.
18. Abetov DA, et al. Formation of mammalian preribosomes proceeds from intermediate to composed state during ribosome maturation. J Biol Chem. 2019;294(28):10746-57.
19. Louis-Andre Julien, et al. mTORC1-activated S6K1 phosphorylates Rictor on threonine 1135 and regulates mTORC2 signaling. Mol Cell Biol. 2010;30(4):908-21.
20. Bartley CM, et al. FMRP S499 is phosphorylated independent of mTORC1-S6K1 activity. PLoS One. 2014;9(5):e96956.
21. Maiuri MC, et al. Autophagy regulation by p53. Curr Opin Cell Biol. 2010;22(2):181-5.
22. Ravanan P, et al. Autophagy: the spotlight for cellular stress responses. Life Sci. 2017;188:53–67.
23. Czekanska EM, et al. In search of an osteoblast cell model for in vitro research. Eur Cell Mater. 2012;24:1-17.
24. Lu Z, et al. ARHI (DIRAS3) induces autophagy in ovarian cancer cells by downregulating the epidermal growth factor receptor, inhibiting PI3K and Ras/MAP signaling and activating the FOXo3a-mediated induction of Rab7. Cell Death Differ. 2014;21(8):1275-89.
25. Triplett JC, et al. Age-related changes in the proteostasis network in the brain of the naked mole-rat: Implications promoting healthy longevity. Biochim Biophys Acta. 2015;1852(10 Pt A):2213-24.
26. Xie Y, et al. PI3K/Akt signaling transduction pathway, erythropoiesis and glycolysis in hypoxia (Review). Mol Med Rep. 2019;19(2):783-91.

27. Liu Q, et al. Akt and mTOR mediate programmed necrosis in neurons. Cell Death Dis. 2014;5(2):e1084.
28. Bakker AD, et al. Mechanical stimulation and IGF-1 enhance mRNA translation rate in osteoblasts via activation of the AKT-mTOR pathway. J Cell Physiol. 2016;231(6):1283-90.
29. Chen Y, et al. Recent progress in autophagic lysosome reformation. Traffic. 2017;18(6):358-61.
30. Chen Y, et al. Development of research into autophagic lysosome reformation. Mol Cells. 2018;41(1):45-9.
31. Tang D, et al. The molecular machinery of regulated cell death. Cell Res. 2019;29(5):347-64.
32. Mizushima N, et al. Protein turnover via autophagy: implications for metabolism. Annu Rev Nutr. 2007;27:19-40.
33. Tong X, et al. Osteoprotegerin inhibit osteoclast differentiation and bone resorption by enhancing autophagy via AMPK/mTOR/p70S6K signaling pathway in vitro. J Cell Biochem. 2018;120:1630-42.
34. Pesce Viglietti AI, et al. *B. Abortus* modulates osteoblast function through the induction of autophagy. Front Cell Infect Microbiol. 2018;8:425.
35. Yang A, et al. Semisynthetic lipidated LC3 protein mediates membrane fusion. ChemBioChem. 2013;14(11):1296-300.
36. Brauer A, et al. Osteogenic differentiation of immature osteoblasts: Interplay of cell culture media and supplements. Biotech Histochem. 2016;91(3):161-9.

Figures

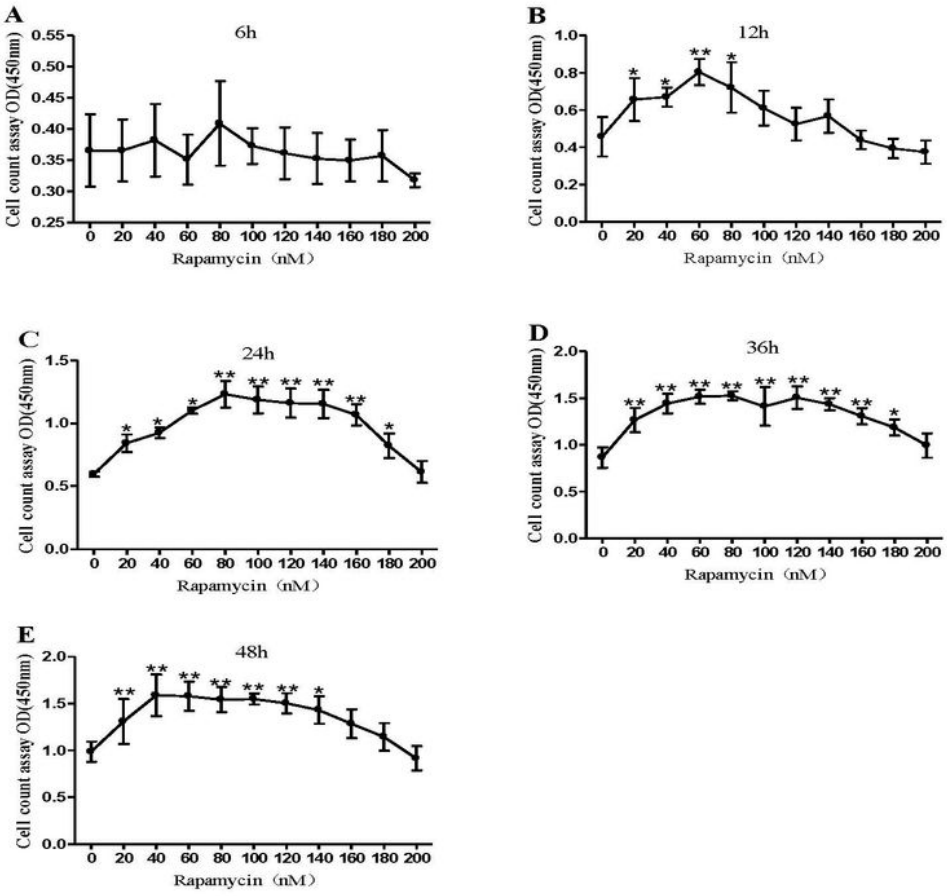

Figure 1

Effects of rapamycin on MC3T3-E1 cell viability. MC3T3-E1 cells were seeded in 96-well plate and then were exposed to 20, 40, 60, 80, 100, 120, 140, 160 and 200 nM rapamycin for 6, 12, 24, 36, and 48 hours. Cells in the control group were cultured with α-MEM (rapamycin -free) for the same period. The Cell Counting Kit-8 (CCK-8) was used to determine the number of viable cells under different experimental condition. Absorbance was measured at 450 nm in a spectrophotometer. Average optical density (OD)

value of cell viability was represented as the mean ± standard deviation. Significance analysis of the experimental data for each group was performed using one-way analysis of variance and Tukey's multiple comparisons test (n=8). *p<0.05, **p<0.01 vs. control group.

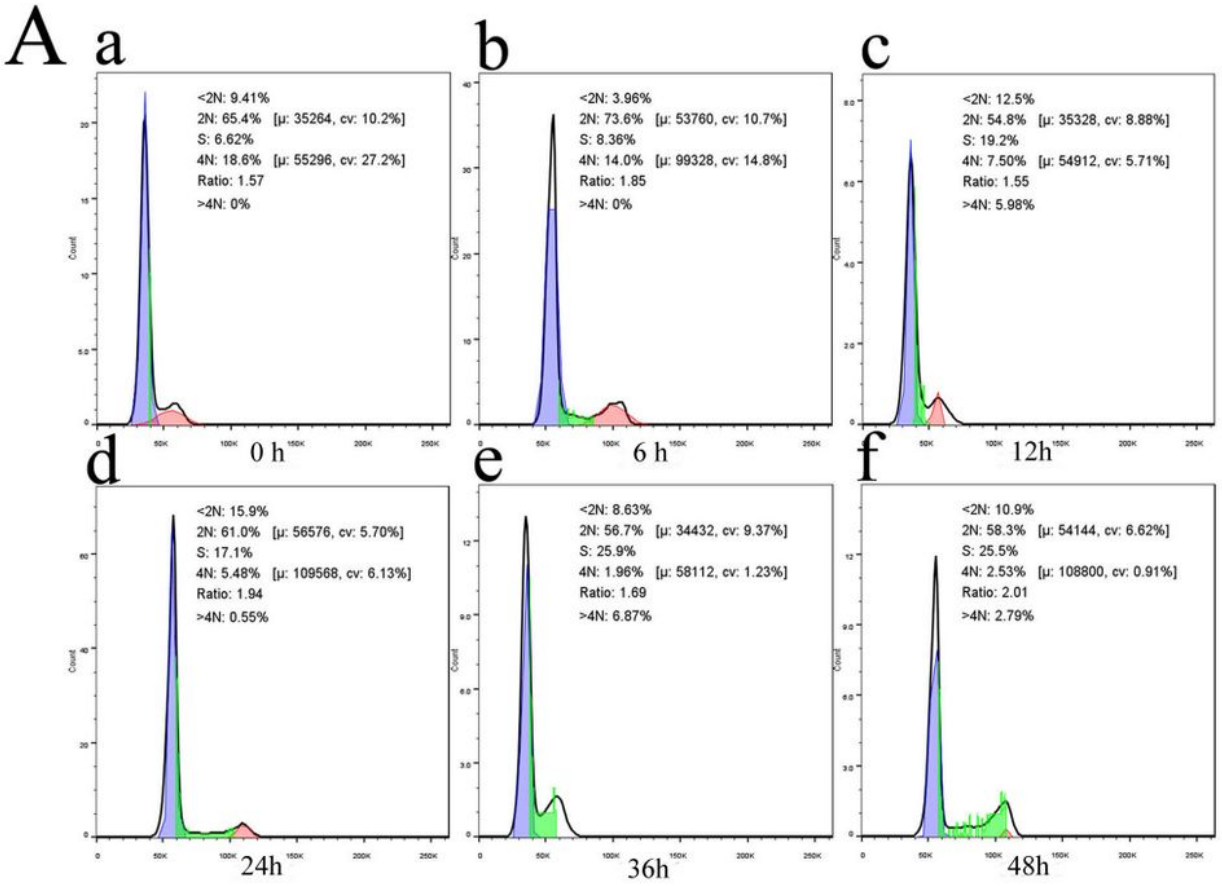

Figure 2

Effects of rapamycin on MC3T3-E1 cell cycle. Cells were treated with 50 nM rapamycin for 6, 12, 24, 36, and 48 hours as induction groups. Cells in the control group were cultured with α-MEM (rapamycin-free)

for the same period. (A) Cell cycle analysis using flow cytometry following PI staining and (B) quantification of the cell cycle populations demonstrated that the proportion of cells in G0/G1, S and G2/M phases changed in the rapamycin treatment group compared with that in the control. Values are expressed as the mean ± standard deviation (n=3). *p<0.05, **p<0.01 vs. respective control group.

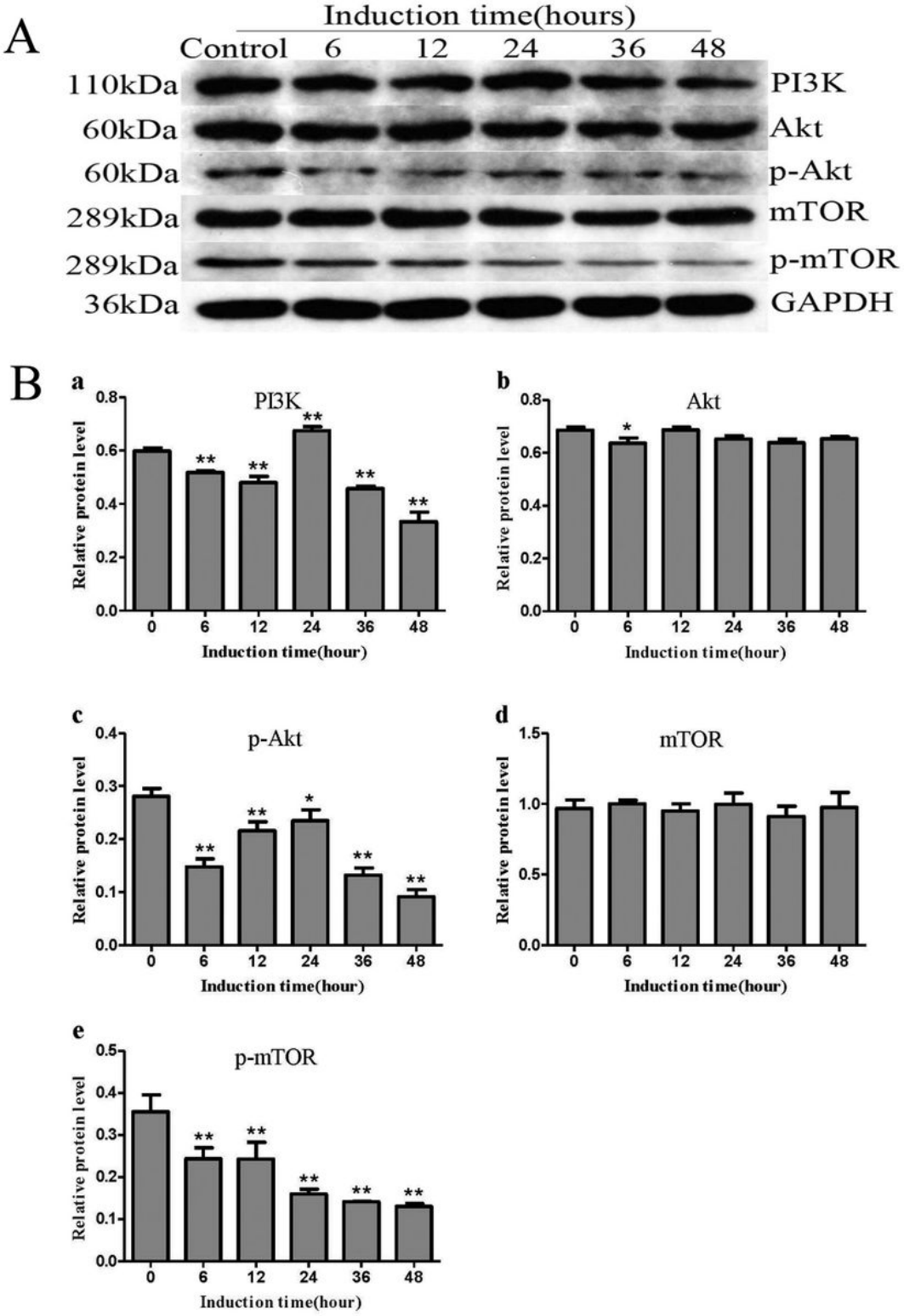

Figure 3

The relative protein levels of PI3K/Akt/mTOR signaling pathway in MC3T3-E1 cells exposed to rapamycin. Cells were treated with 50 nM rapamycin for 6, 12, 24, 36, and 48 hours. Cells in the control group were cultured with α-MEM (rapamycin-free) for the same period. Cells were harvested with cell lysis buffer. Whole-cell extracts from MC3T3-E1 cells were separated on SDS-PAGE for Western blot analysis using antibody specific to phosphorylation of mammalian target of rapamycin (p-mTOR), protein kinase B (Akt), p-Akt and phosphatidylinositol 3'-kinase (PI3K). Data shown are the mean ± SD (n=3). *p<0.05, **p<0.01 vs. respective control group.

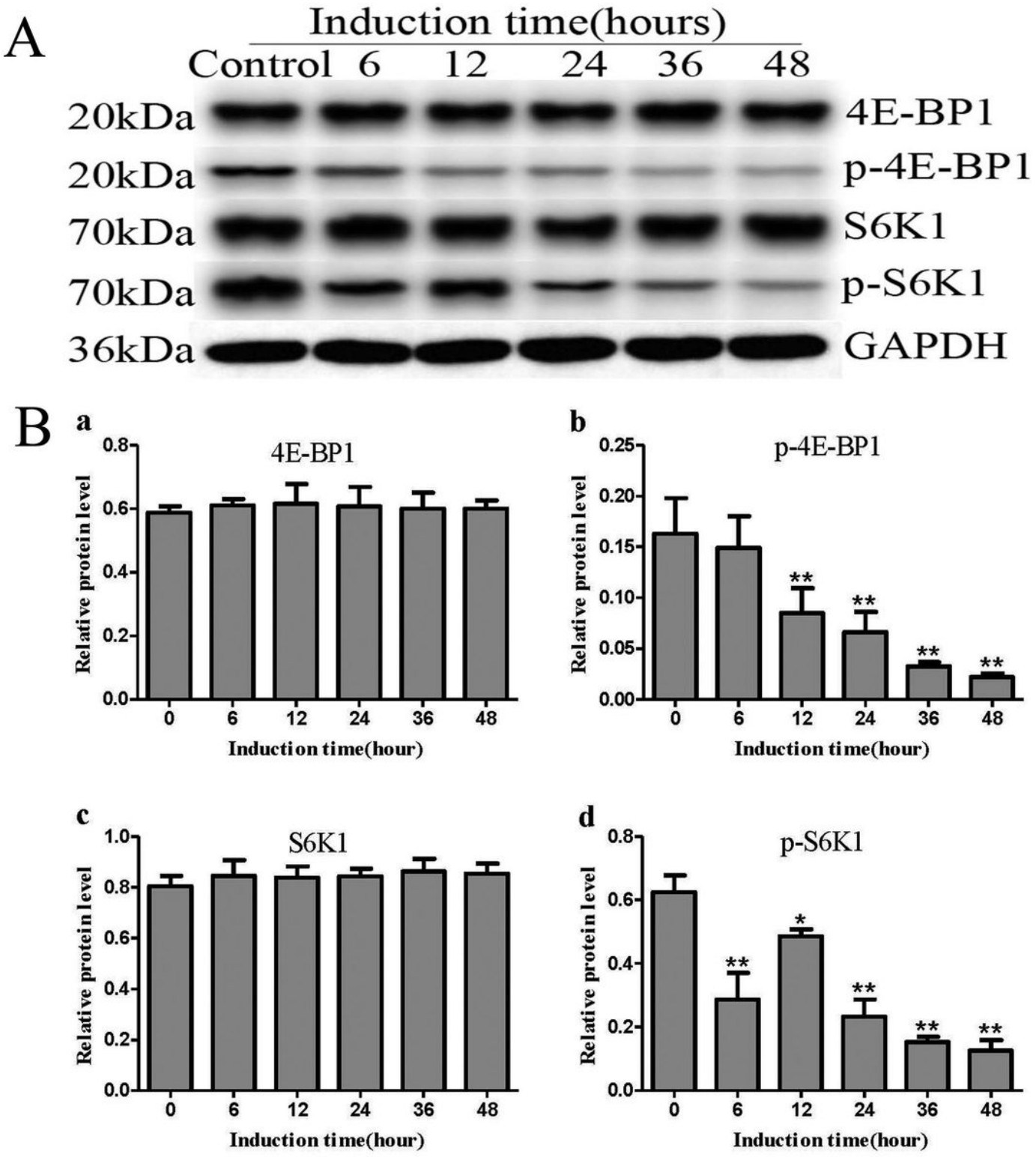

Figure 4

The relative protein levels of mTOR signaling pathway in MC3T3-E1 cells exposed to rapamycin. Cells were treated with 50 nM rapamycin for 6, 12, 24, 36, and 48 hours. Cells in the control group were cultured with α-MEM (rapamycin-free) for the same period. Cells were harvested with cell lysis buffer. Whole-cell extracts from MC3T3-E1 cells were separated on SDS-PAGE for Western blot analysis using antibody specific to eIF4E-binding protein 1 (4E-BP1), p-4E-BP1, p70 ribosomal S6 kinase 1 (S6K1) and p-S6K1. Data shown are the mean ± SD (n=3). *p<0.05, **p<0.01 vs. respective control group.

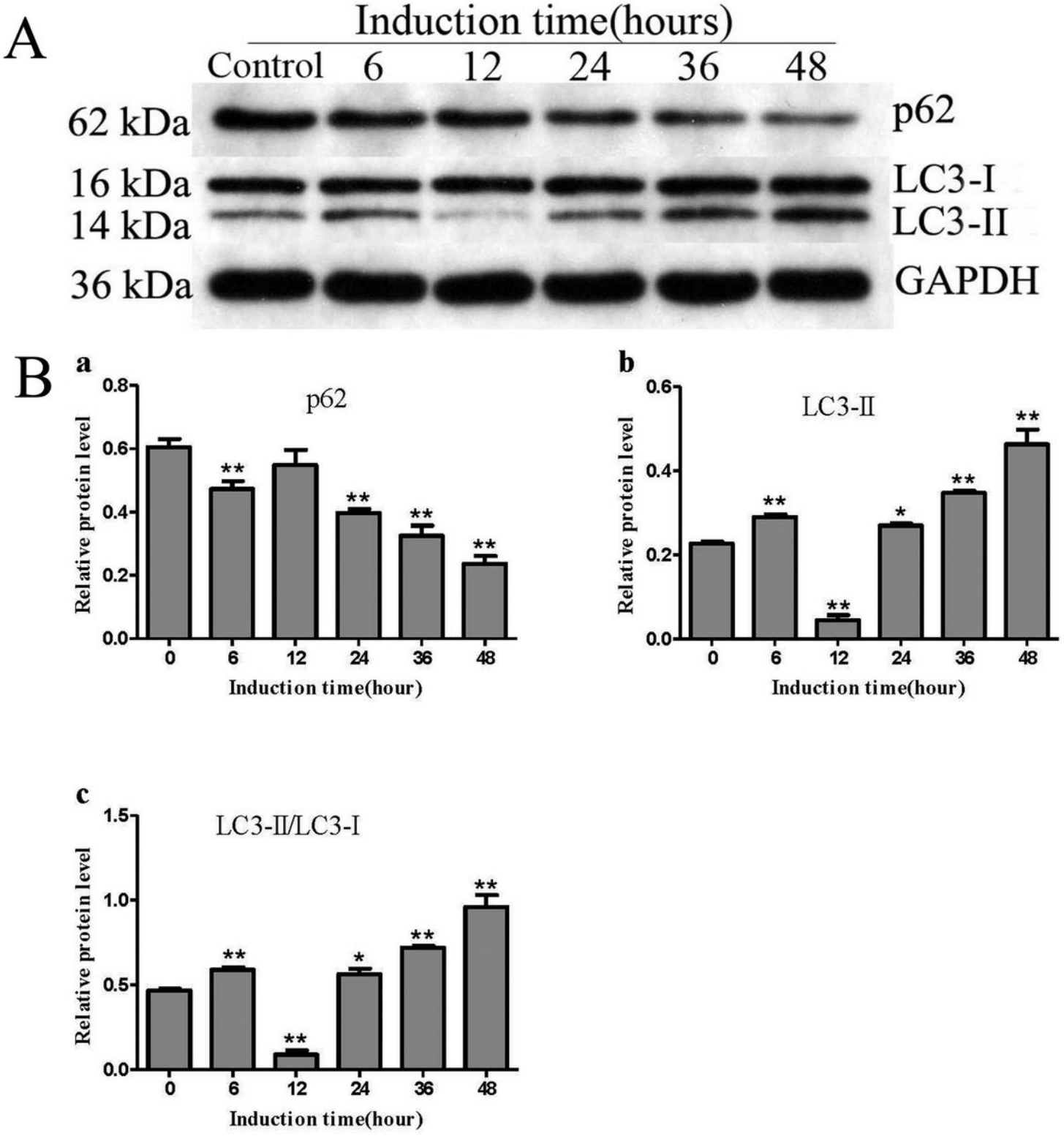

Figure 5

The relative protein levels of autophagy in MC3T3-E1 cells exposed to rapamycin. Cells were treated with 50 nM rapamycin for 6, 12, 24, 36, and 48 hours as induction groups. Cells in the control group were cultured with α-MEM (rapamycin-free) for the same period. Cells were harvested with cell lysis buffer. Whole-cell extracts from MC3T3-E1 cells were separated on SDS-PAGE for Western blot analysis using antibody specific to Sequestosome1 (p62) and microtubule associated protein 1 light chain 3-α (LC3-II). Data shown are the mean ± SD (n=3). *p<0.05, **p<0.01 vs. respective control group.

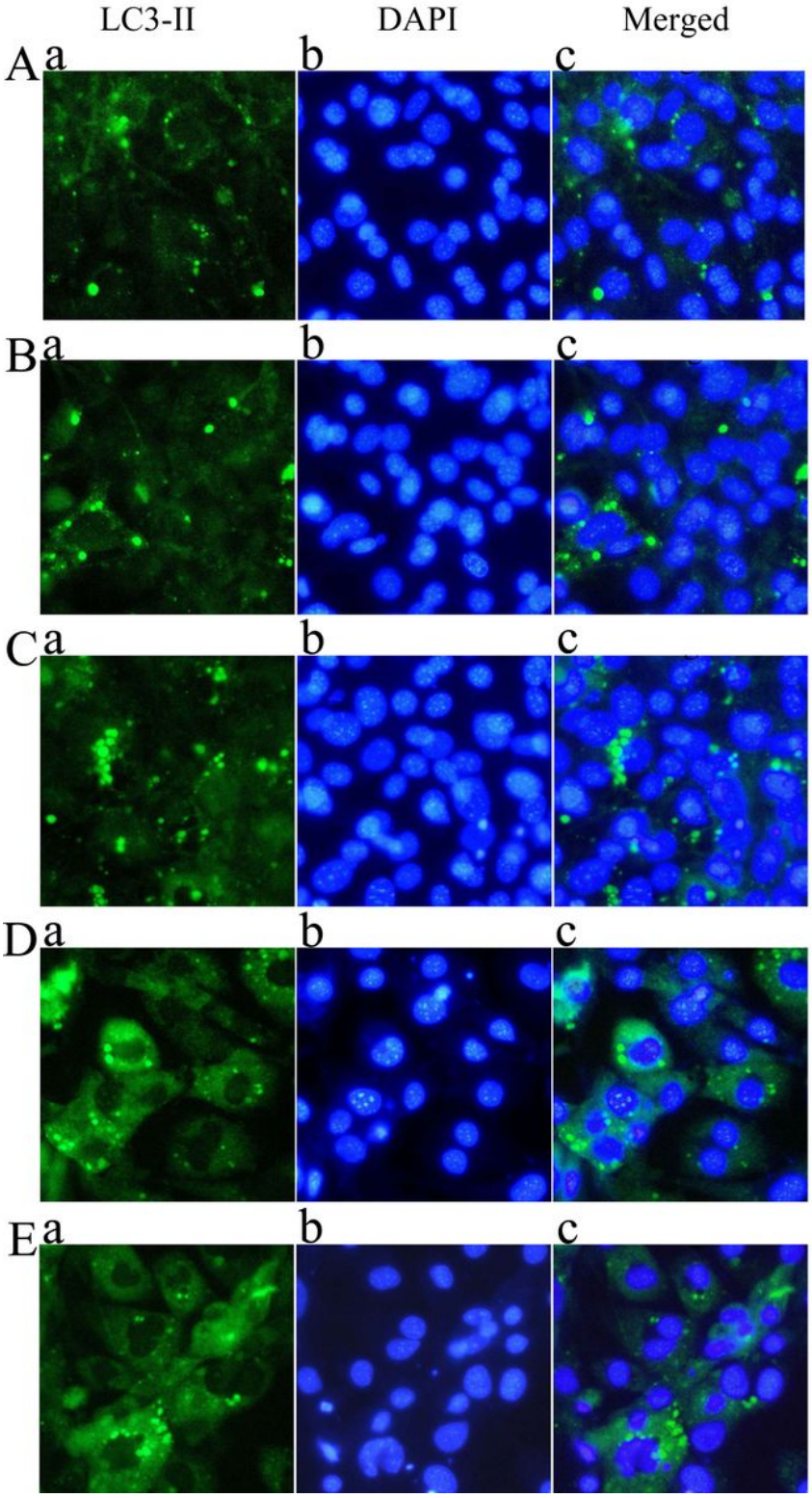

Figure 6

Representative images for protein expression of LC3-II in MC3T3-E1 cells exposed to rapamycin with immunofluorescence staining. Cells were treated with 50 nM rapamycin for 12 (B), 24 (C), 36 (D), and 48 hours (E) as induction groups. Cells in the control group (A) were cultured with α-MEM (rapamycin-free) for the same period. Cells were stained in situ with fluorescence of FITC labeled anti-LC3-II, and DAPI staining was carried out as described in cell nucleus. Cells showed fluorescence intensity changes of LC3-II antibody positive staining in their cytoplasm from control group under microscopy (magnification, ×200).

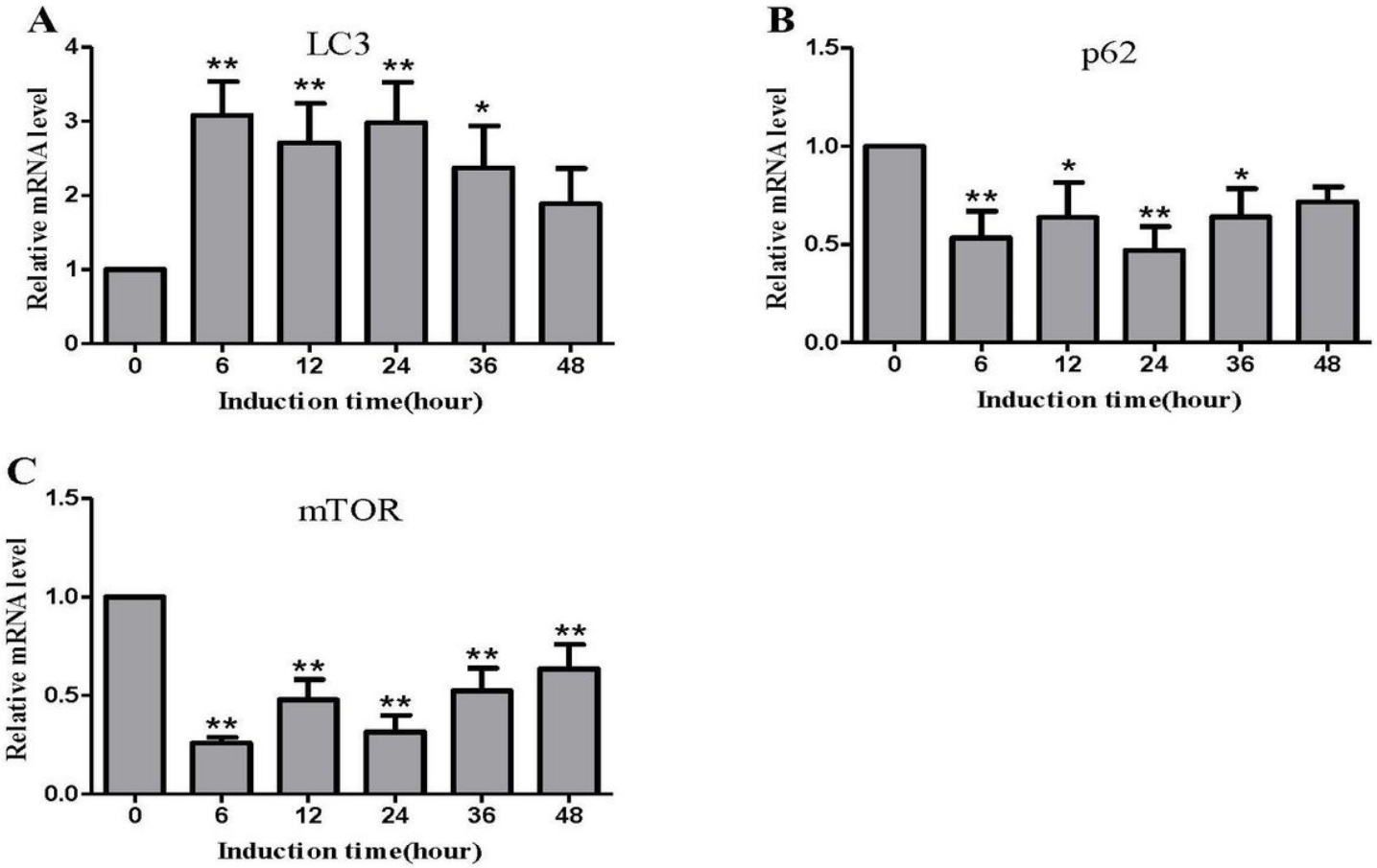

Figure 7

The relative RNA abundance of autophagy signaling pathway in MC3T3-E1 cells exposed to rapamycin. Cells were treated with 50 nM rapamycin for 6, 12, 24, 36, and 48 hours as induction groups. Cells in the control group were cultured with α-MEM (rapamycin-free) for the same period. Quantitative PCR was performed with an SYBR Green PCR Master Mix. Average relative RNA abundance of immunoglobulim heavy chain LC3-II, p62 and mTOR are represented as mean ± SD (n=3). *p<0.05, **p<0.01 vs. respective control group.

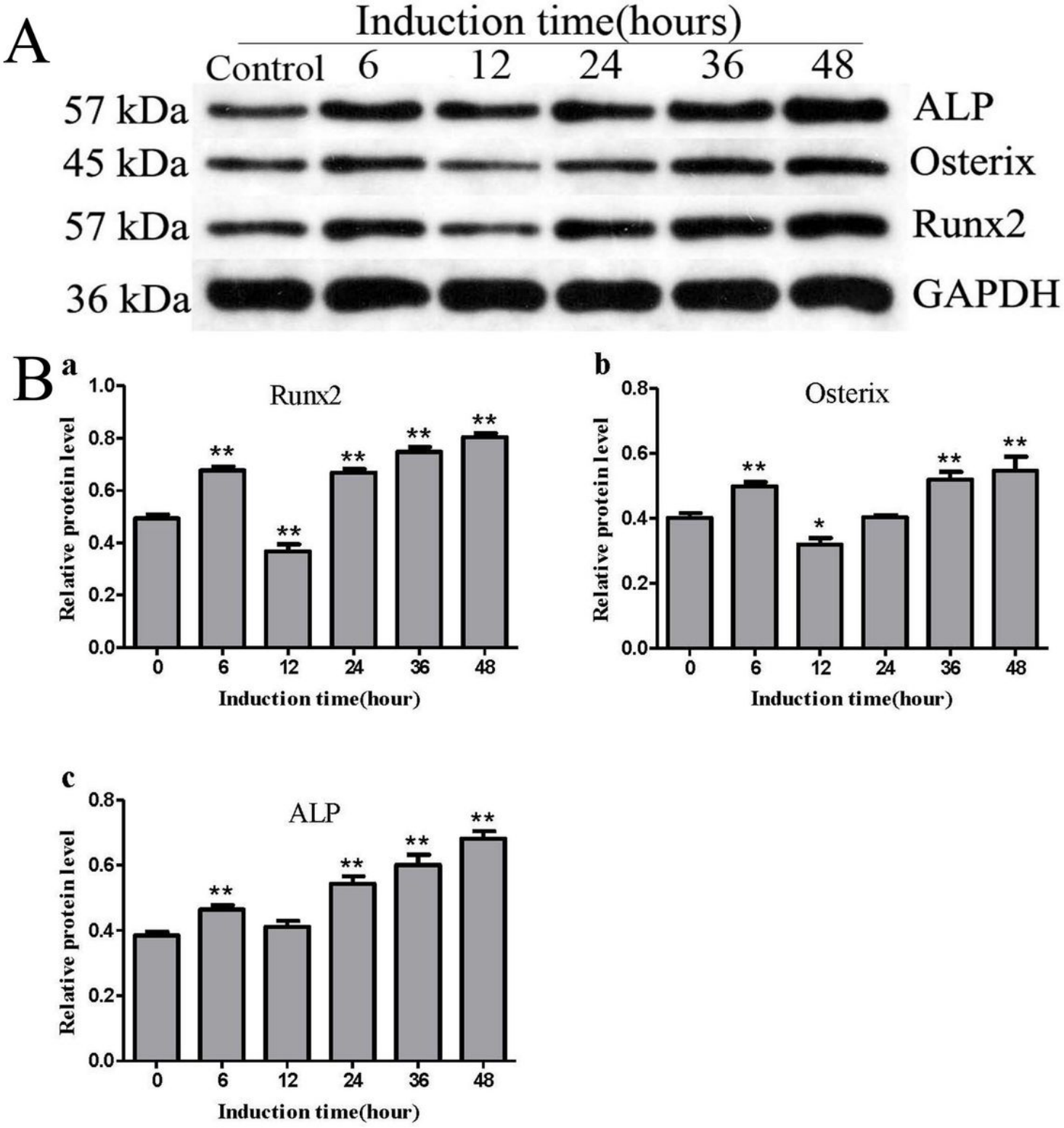

Figure 8

The relative protein levels of transcription factors related to osteoblast differentiation in MC3T3-E1 cells exposed to rapamycin. Cells were treated with 50 nM rapamycin for 6, 12, 24, 36, and 48 hours as induction groups. Cells in the control group were cultured with α-MEM (rapamycin-free) for the same period. Cells were harvested with cell lysis buffer. Whole-cell extracts from MC3T3-E1 cells were separated on SDS-PAGE for Western blot analysis using antibody specific to Runt-related transcription

factor 2 (Runx2), osterix and alkaline phosphatase (ALP). Data shown are the mean ± SD (n=3). *p<0.05, **p<0.01 vs. respective control group.

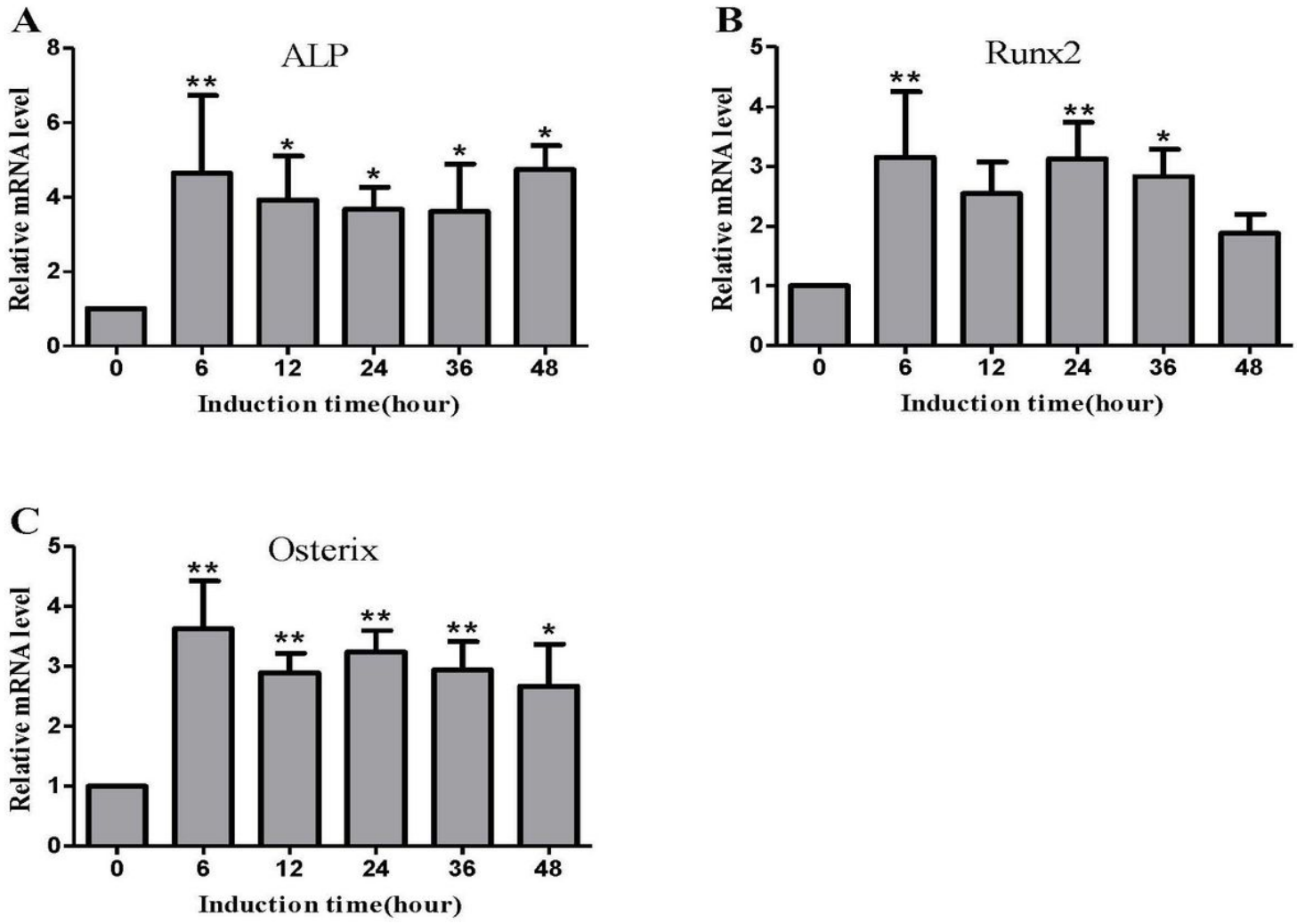

Figure 9

The relative RNA abundance of transcription factors related to osteoblast differentiation in MC3T3-E1 cells exposed to rapamycin. Cells were treated with 50 nM rapamycin for 6, 12, 24, 36, and 48 hours as induction groups. Cells in the control group were cultured with α-MEM (rapamycin-free) for the same period. Quantitative PCR was performed with an SYBR Green PCR Master Mix. Average relative RNA abundance of immunoglobulim heavy chain ALP, Runx2 and osterix are represented as mean ± SD (n=3). *p<0.05, **p<0.01 vs. respective control group.

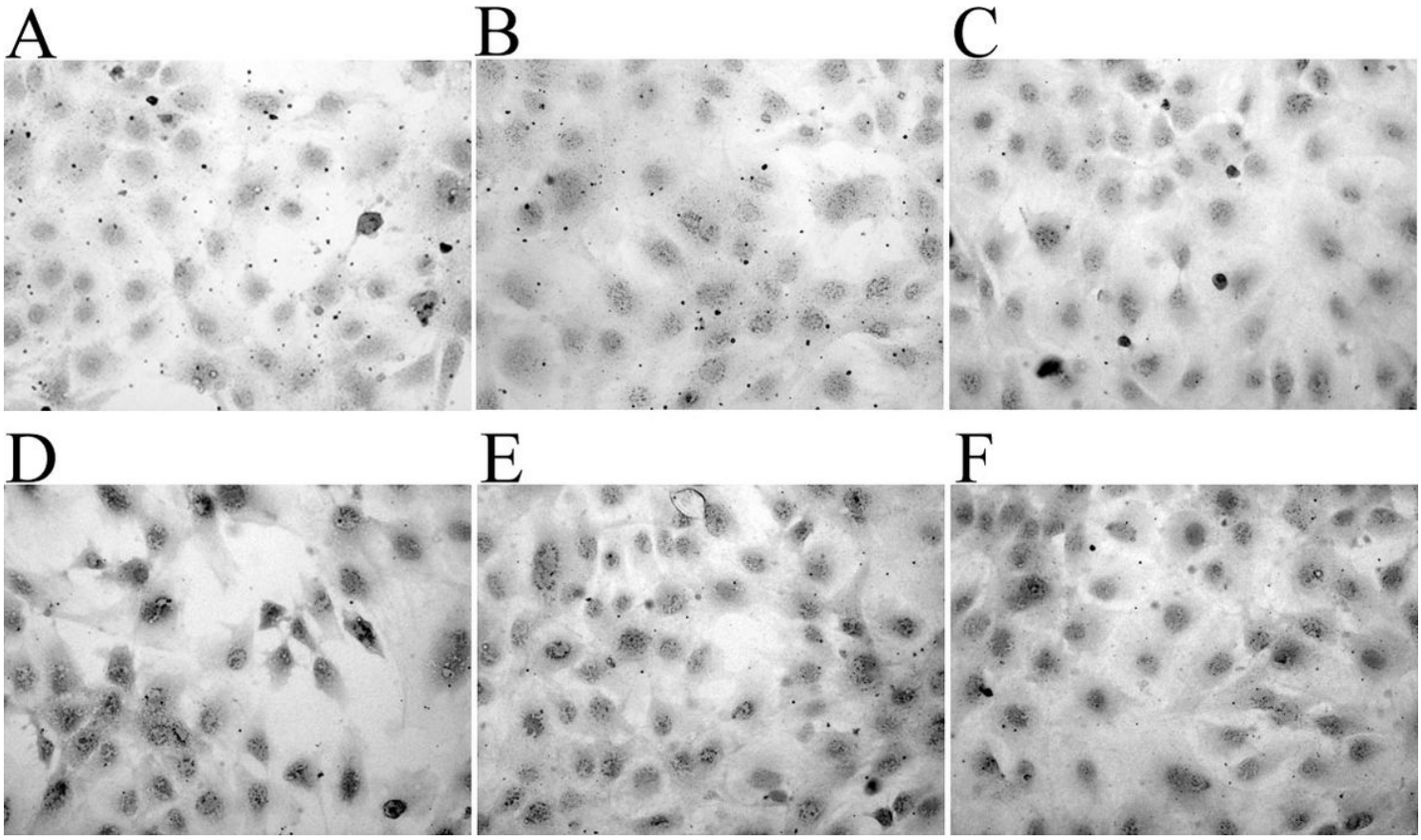

Figure 10

Effects of rapamycin on the activity of alkaline phosphatase in MC3T3-E1 cells. Alkaline phosphatase reaction appeared as gross and microscopic staining of osteoblasts differentiated from MC3T3-E1 cells. Cells were treated with 50 nM rapamycin. The activity of alkaline phosphatase in a microscope slide fixed on 6 (B), 12 (C), 24 (D), 36 (E) and 48 (F) hours and stained with modified Gomori Ca–Co staining. Deposition of Cobalt sulfide particles were showed in cells from control group (A) under microscopy. The Positive reaction indicated that light black (black arrows) to minor granules (red arrows) could be seen in cytoplasm (magnification, ×200).

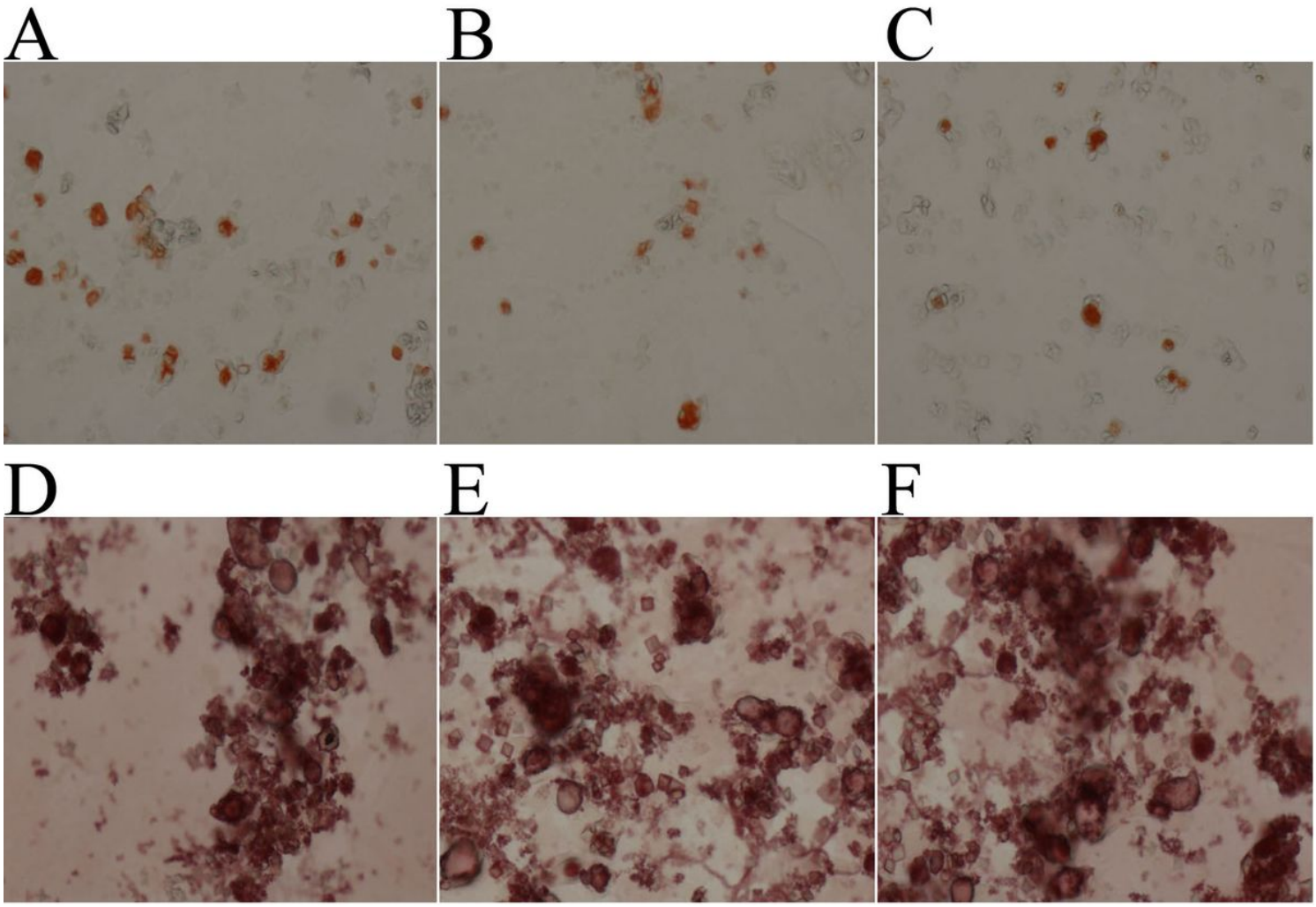

Figure 11

Effects of Rapamycin on formation of mineral nodules in MC3T3-E1 cells. Alizarin red staining appeared as gross and microscopic observation of osteoblasts late differentiated from MC3T3-E1 cells. Positive staining with pink color indicated bone nodule formation (blue arrows). The effect ofRapamycin on the mineralized nodules formation of osteoblast was observed in a microscope slide fixed. Cells were treated with 50 nM Rapamycin. Deposition of calcium salts (red arrows) were showed in cells from control group (A), 2 (B) and 6 days (C), and mineral nodule formation (blue arrow) were showed in cells from 12 (D), 14 (E) and 16 days (F) under microscopy (magnification, ×200).